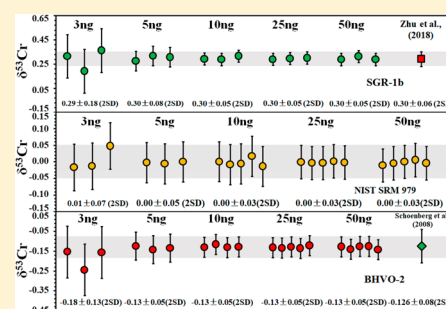


High-Sensitivity Measurement of Cr Isotopes by Double Spike MC-ICP-MS at the 10 ng Level

Guangliang Wu,[†] Jian-Ming Zhu,^{*,†,‡,§,||} Xiangli Wang,^{§,||} Thomas M. Johnson,[⊥] and Guilin Han[†][†]State Key Laboratory of Geological Processes and Mineral Resources, China University of Geosciences (Beijing), Beijing 100083, China[‡]State Key Laboratory of Environmental Geochemistry, Institute of Geochemistry, CAS, Guiyang 550081, China[§]Department of Marine Sciences, University of South Alabama, Mobile, Alabama 36688, United States^{||}Dauphin Island Sea Lab, Dauphin Island, Alabama 36528, United States[⊥]Department of Geology, University of Illinois at Urbana–Champaign, 3081 Natural History Building, Urbana, Illinois 61801, United States

Supporting Information

ABSTRACT: High-sensitivity and high-precision ($2 \text{ SD} \leq 0.06\%$) measurement of chromium (Cr) isotopes at the 10 ng level was successfully carried out using double spike multiple-collector inductively couple plasma mass spectrometry (MC-ICP-MS). To enhance the signal sensitivity and stability, the Aridus II desolvating nebulizer system was improved by placing its waste gas trap bottle in an ice chamber (5°C cold trap). This setup, beyond Cr isotope analysis, can be applied to most heavy metal isotope measurements. The sensitivity of the ^{52}Cr signal is $\geq 300 \text{ V mg}^{-1} \text{ L}$ (with a $10^{11}\Omega$ amplifier and a $110 \mu\text{L min}^{-1}$ uptake rate), an enhancement of ≥ 1.5 times compared to the Aridus II without the cold trap. In addition, the relative standard deviation of the ^{52}Cr signal varied $\leq 4\%$ over 8 h, demonstrating high stability. The $\delta^{53}\text{Cr}$ values of common geological reference materials determined using 10 ng of Cr are in excellent agreement with results measured at 25 ng and 50 ng and are consistent with previous determinations, validating the accurate and precise Cr isotope ratio measurements. An empirical method is proposed to correct for the residual (after subtraction) effect of Fe interference on $\delta^{53}\text{Cr}$ determination. This method relies on a linear relationship between the $[\text{Fe}]/[\text{Cr}]$ and $\delta^{53}\text{Cr}$ shift within one analytical session. Finally, we report the $\delta^{53}\text{Cr}$ values of 19 new reference materials, ranging from -0.44% to 0.49% . Among them, GSS-7 ($-0.44 \pm 0.02\%$, 2 SD , $n = 5$), GSS-4 ($0.48 \pm 0.02\%$, 2 SD , $n = 5$), and GSD-10 ($0.49 \pm 0.05\%$, 2 SD , $n = 5$) can be used as candidate reference materials for interlaboratory comparisons to complement existing ones that are mostly isotopically unfractionated from the bulk silicate earth.



Carbonate rock (Cr concentration: $0.008\text{--}29 \mu\text{g g}^{-1}$ with a median value of $1.93 \mu\text{g g}^{-1}$),^{20–25} river/seawater (Cr concentration: $57\text{--}1390 \text{ ng kg}^{-1}$ with a median value of 157 ng kg^{-1}),^{20–22,26–34} intermediate and felsic magmatic rock (Cr concentration: $0.01\text{--}101 \mu\text{g g}^{-1}$ with a median value of $6.0 \mu\text{g g}^{-1}$),^{35–37} and other samples with lower Cr content³⁸ play an irreplaceable role in improving our understanding of paleo-environment evolution and the global Cr cycle.^{20–34,39–43} Although the Cr mass required per analysis has been reduced to 100 ng for obtaining high precision data ($2 \text{ SD} \leq 0.06\%$),⁶ large sample masses must be prepared and purified for obtaining high-precision Cr isotopic composition of low-Cr samples. This not only decreases the experimental efficiency⁴⁴ but also easily leads to low yield and undesirable matrix effects.⁹

INTRODUCTION

Chromium (Cr) is a group VI-B element located in the fourth period of the periodic table, and it is a typical transition metal with four stable isotopes (^{50}Cr , ^{52}Cr , ^{53}Cr , and ^{54}Cr).¹ Early determination of Cr isotopes was performed on single-focusing solid-source thermal ionization mass spectrometers (TIMS) with $0.2\text{--}60 \mu\text{g}$ of Cr consumed per analysis, with precisions ranging from 0.20% to 1.5% .^{2–4} In the past 10 years, with the development and improvement of multiple-collector thermal ionization mass spectrometers (MC-TIMS) and multiple-collector inductively coupled plasma mass spectrometers (MC-ICP-MS), the precision of Cr isotope composition measurement ($^{53}\text{Cr}/^{52}\text{Cr}$) has been improved to $0.01\text{--}0.08\%$ (2 SD), and the required Cr mass for a single measurement has decreased to $0.1\text{--}2 \mu\text{g}$.^{5–10} Benefiting from these technological advancements, Cr isotopes are increasingly used as a powerful tool for reconstructing paleo-ocean redox evolution and identifying the sources and transport pathways of Cr contamination in groundwater.^{4,11–19}

Received: October 15, 2019
Accepted: November 26, 2019
Published: November 26, 2019

In order to obtain precise Cr isotope compositions of extremely low-Cr samples, two approaches can be taken: (1) purify Cr from large amounts of samples with low blank and/or (2) measure it precisely on the instrument using a small amount of Cr. Chromium blank has been reduced to 0.12–0.20 ng by Bonnand et al.⁶ and Li et al.⁴⁵ Therefore, we aimed to tackle the second problem in this paper. Some studies have attempted to measure Cr isotopes at the 10 ng level using double spike MC-ICP-MS⁴³ and MC-TIMS.⁴⁶ Although an accurate isotope ratio was successfully achieved, the precision was 0.26‰ (2 SD)⁴³ and 0.20‰ (2 SD),⁴⁶ respectively. These precisions were insufficient if one wants to resolve smaller isotope variations that are often found in studies of various biogeochemical processes.

Given the wide range of sample types investigated in this work, we adopted our earlier method that is capable of handling such a variety of samples.⁹ Since our method can achieve a Cr blank of 0.8 ± 0.1 ng (2 SD, $n = 4$), in order to avoid interference of the blank with our low-Cr measurement, samples containing 200–300 ng of Cr were employed to extract Cr by a universal separation scheme, and purified sample solutions were diluted to very low concentrations during measurement so as to test a simple technique for determining high-precision and -accuracy Cr isotope composition using double spike (⁵⁰Cr–⁵⁴Cr) MC-ICP-MS at the 5–10 ng level. In this simple yet powerful technique, the Aridus II desolvating nebulizer system is improved by cooling the waste gas condensation bottle to achieve a high sensitivity and stability. The external precision is ≤ 0.06 ‰ (2 SD) and 0.08‰ (2 SD) when the concentration of analyte is ≥ 10 $\mu\text{g L}^{-1}$ and 5 $\mu\text{g L}^{-1}$, respectively. Meanwhile, an empirical method is established to provide a secondary correction for Fe interferences that could not be completely corrected for by previously used Fe correction methods when the $[\text{Fe}]/[\text{Cr}]$ ratio is greater than 0.1. This secondary correction is based on a well-tested empirical, linear relationship between $[\text{Fe}]/[\text{Cr}]$ and $\delta^{53}\text{Cr}$. These results show that high-precision measurement of the Cr isotope ratio at the 5–10 ng level can be carried out in many common laboratories with an MC-ICP-MS using our proposed cold trap for Aridus II/III.

EXPERIMENTAL DETAILS

Reagents, Materials, and Sample Preparation. The optima-grade HF, HCl, and HNO₃ were purchased from the Beijing Institute of Chemical Reagents and further purified once for HF and twice for HCl and HNO₃ by a sub-boiling distillation system (DST-4500, Savillex). Ultrapure water (MQ) with a resistivity of 18.2 M Ω cm⁻¹ was prepared from a Milli-Q Element system (Millipore, U.S.A.). Hydroxylamine hydrochloride (NH₂OH·HCl, 99.995%), NH₃·H₂O (99.999%), H₂O₂ (35%, wt./wt., guarantee reagent grade), (NH₄)₂S₂O₈ (99.8%), and single element standard solutions (Ti, Fe, and V etc.) were obtained from Alfa Aesar. The Cr isotope standard (SRM 979) was purchased from the National Institute of Standards and Technology (NIST). Ion exchange resins (AG50W-X8, 200–400 mesh; AG1-X8, 100–200 mesh and 200–400 mesh) and 10 mL polypropylene columns were purchased from Bio-Rad (U.S.A.). Fifteen milliliter PFA beakers, pipet tips, and 7 mL tubes were cleaned with 50% (v/v) HNO₃, 10% (v/v) HNO₃, and 4 M HCl, and they were air-dried in a class-100 hood installed in a class-1000 room.⁹ The calibration method and composition of the double spike (⁵⁰Cr–⁵⁴Cr) were detailed in our previous study.⁹

Twenty-two geological reference materials (GRMs) were measured in this paper. BHVO-2 (basalt) and SGR-1b (shale) were purchased from the United States Geological Survey (USGS); JP-1 (peridotite) was acquired from the Geological Survey of Japan (GSJ). The Cr isotope compositions of these GRMs are widely used to compare measured results among laboratories. The GRMs of igneous and sedimentary rocks (GSR-1, -2, -4–6), soils (GSS-1–7, ESS-1), and stream sediments (GSD-1, -3, -9, -10, -11, -12) were purchased from the Institute of Geophysical and Geochemical Exploration (IGGE), China. The concentrations of Cr and collection locations are listed in Table S1.

The digestion procedures for different types of samples were presented in detail in Zhu et al.⁹ Briefly, ~50 mg of powdered igneous samples was digested using mixed HNO₃–HF (HNO₃/HF = 1:2) and *Aqua regia* (HCl/HNO₃ = 3:1) in 15 mL PFA beakers. Other samples including soils, stream sediments, and sedimentary rocks were digested using customized high-pressure bombs. About 100 mg of powdered samples was decomposed with 3 mL of mixed HNO₃–HF (HNO₃/HF = 4:1) and heated at 185 ± 5 °C for more than 36 h. The completely digested samples were dissolved in 2 M HNO₃ mixed with 0.5% (v/v) H₂O₂ and stored for 5 days before Cr purification.⁹

The purification of all samples was conducted in a class 100 hood in the Laboratory of Surficial Environmental Geochemistry, China University of Geosciences (Beijing). Similar to previous studies,^{4,5} the double spike was used to correct the potential isotope fractionations of chemical separation and measurement. Sample solutions containing 200–300 ng of Cr were spiked with a suitable volume of the double spike (DS) to achieve a ratio of $^{54}\text{Cr}_{\text{spike}}/^{52}\text{Cr}_{\text{sample}} \sim 0.4$.⁹ The spiked sample solutions were sealed in PFA beakers and heated overnight at 100 °C to allow for spike–sample equilibration. The Cr separation from sample matrix elements was achieved using a three-step ion exchange scheme, following procedures presented in Zhu et al.⁹ (Table S2). The resins were preloaded in polypropylene columns (10 mL, Bio-Rad Company), cleaned, and conditioned. According to procedures in step I, the spiked samples were sequentially passed through 2 mL of AG50W-X8 (200–400 mesh) and 2 mL of AG1-X8 (100–200 mesh) resins to remove Fe and Ca. Ti and V were eliminated by passing samples through 1 mL of the AG1-X8 (200–400 mesh) resin described in step II. Step III was used to separate Cr from the remaining matrix elements. In step III, Cr(III) in samples was oxidized to Cr(VI) by (NH₄)₂S₂O₈ at neutral pH (adjusted with NH₃·H₂O). After removing precipitated solids by centrifugation, the supernatants were passed through 2 mL of AG1-X8 (100–200 mesh) columns to obtain high-purity Cr. Purified Cr samples were redissolved in 2% HNO₃ and diluted to target concentrations: 50 $\mu\text{g L}^{-1}$, 25 $\mu\text{g L}^{-1}$, 10 $\mu\text{g L}^{-1}$, and 5 $\mu\text{g L}^{-1}$ (only for SRM979, BHVO-2, and SGR-1b) for isotope measurement.

Improvement of a Desolvating Nebulizer System. Aridus II (Cetac, U.S.A.) as a sample introduction system can enhance analyte sensitivity and significantly reduce the occurrence of solvent-based interference by effectively separating analytes and solvent.^{47,48} Importantly, a 15 L trap bottle is used to condense the solvent vapor carried in the “sweep gas” waste stream coming out of the heated chambers of the Aridus II device. Due to the relatively high and temporally variable temperature of the trap bottle, its pressure is very susceptible to external conditions such as indoor

temperature and air pressure. The change of the pressure in the waste gas trap bottle adversely affects the sweep gas and further influences the signal sensitivity and stability.⁴⁷ In order to solve this problem, the trap bottle was mounted in a sealed ice chamber. The ice chamber consisted of an incubator and ice bags as shown in Figure 1. The volume of the incubator was

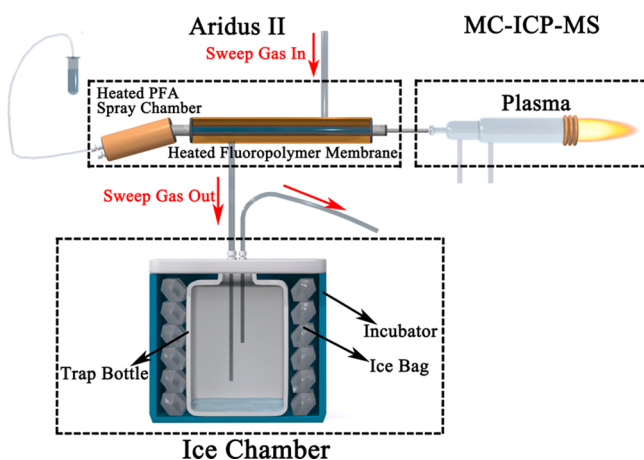


Figure 1. A schematic drawing of the improved Aridus II with an ice chamber.

~34 L, and the trap bottle was placed in the middle of the incubator and surrounded by 12 ice bags, which maintained the temperature of the sealed incubator at approximately 5 °C for more than 10 h between ice bag replacements. Waiting 30 min after replacing ice bags, the gas flows of the instrument and Aridus II were fine-tuned to achieve optimal signal intensity and stability.

Mass Spectrometer. The Cr isotope measurements were conducted on an MC-ICP-MS (ThermoFisher Scientific Neptune Plus) at the Isotope Geochemistry Laboratory, China University of Geosciences (Beijing). The instrument is equipped with nine Faraday cups; each of the cups is connected to a $10^{11} \Omega$ amplifier. All measurements were conducted in the medium resolution mode using the improved Aridus II equipped with an ice chamber and a $110 \mu\text{L min}^{-1}$ microconcentric PFA nebulizer (ESI, U.S.A.) as the sample introduction system. Other typical operating conditions of the instrument such as gas flow rates, cup configuration, cones, and resolution mode are summarized in Table 1.

Following previously published methods,⁹ all signals including Cr isotopes, ^{49}Ti , ^{51}V , and ^{56}Fe were collected in the center of the left peak plateau (Figure 2) to avoid potential polyatomic interferences such as $^{40}\text{Ar}^{12}\text{C}^+$, $^{40}\text{Ar}^{14}\text{N}^+$, and $^{40}\text{Ar}^{16}\text{O}^+$ on $^{52}\text{Cr}^+$, $^{54}\text{Cr}^+$, and $^{56}\text{Fe}^+$. Each measurement consisted of three blocks, each block with 20 cycles in the static mode. The integration time for each cycle was 4.19 s, followed by a 3 s idle time. The sample take-up time was 80 s, and the total measurement time was 9 min. With an injecting concentration of $10 \mu\text{g L}^{-1}$, the amount of Cr required for one measurement was $\sim 10 \text{ ng}$ ($110 \mu\text{L min}^{-1} \times 9 \text{ min} \times 10 \mu\text{g L}^{-1}$). The on-peak instrument and acid matrix blank were subtracted from the signal intensities. All results were reported relative to SRM 979 as δ (‰): $\delta^{53}\text{Cr} = [(^{53}\text{Cr}/^{52}\text{Cr})_{\text{sample}} / (^{53}\text{Cr}/^{52}\text{Cr})_{\text{SRM 979}} - 1] \times 1000$.

Every five samples were bracketed by a spiked SRM 979 with comparable Cr concentrations to monitor the instrumental stability and normalize the measured ratio of actual

Table 1. Instrument Parameters

parameters	dry plasma
cup configuration	L3 (^{49}Ti), L2 (^{50}Ti , ^{50}V , ^{50}Cr), L1 (^{51}V), C (^{52}Cr), H1 (^{53}Cr), H2 (^{54}Fe , ^{54}Cr), H4 (^{56}Fe)
inlet system	
cool gas	15 L min^{-1}
aux gas	$0.85\text{--}1.03 \text{ L min}^{-1}$
sample gas	$0.90\text{--}1.05 \text{ L min}^{-1}$
RF power	1250 W
cones	sample cone (H type, Ni), skimmer cone (X type, Ni)
resolution mode	medium M/ $\Delta\text{M} \geq 6500$
sample uptake	$110 \mu\text{L min}^{-1}$
Aridus II	
spray chamber temperatures	$110 \text{ }^\circ\text{C}$
desolvator temperatures	$160 \text{ }^\circ\text{C}$
Ar sweep gas	$5\text{--}6 \text{ L min}^{-1}$
nitrogen gas	no
signal sensitivity of ^{52}Cr	$\geq 300 \text{ V } \mu\text{g}^{-1} \text{ mL}$

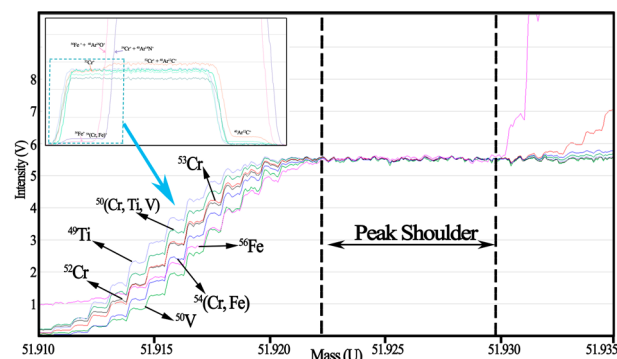


Figure 2. A peak shape at medium resolution. Cr, Ti, and Fe isotopes were measured at the flat region of the peak shoulder.

sample by $\delta^{53}\text{Cr} = \delta^{53}\text{Cr}_{\text{sample}} - \delta^{53}\text{Cr}_{\text{SRM 979}}$. However, the measured $\delta^{53}\text{Cr}_{\text{SRM 979}}$ varied less than 0.1‰ between different sessions.

RESULTS AND DISCUSSION

Sensitivity and Stability. Excellent signal sensitivity and stability are a prerequisite for obtaining high-quality data for samples containing very little Cr. Sensitivity is dependent on sample purity, ion formation efficiency, as well as sample and ion transmission efficiency in the mass spectrometer.⁴⁹ In this study, the sensitivity of ^{52}Cr was $\geq 300 \text{ V mg}^{-1} \text{ L}$ using the improved Aridus II with an ice chamber as the sample introduction system. It is significantly increased in comparison with the previously reported $20\text{--}180 \text{ V mg}^{-1} \text{ L}$ for Aridus II,^{6,50} $7.2\text{--}30 \text{ V mg}^{-1} \text{ L}$ for Apex IR or Spiro,^{10,39} and $2\text{--}15 \text{ V mg}^{-1} \text{ L}$ for wet plasma (stable introduction system;^{9,51} Table S3). The trap bottle is located in a sealed 5 °C ice chamber to accelerate the condensation of sweep gas and thus reduce the pressure of the bottle, allowing the solvent vapor to be more readily swept away by argon gas. As the solvent content decreases, the transmission efficiency of the analyte is increased to enhance the signal sensitivity.⁵² On the other hand, a stable signal is essential for collecting highly precise data.⁵³ Under optimized conditions, the signal intensity of ^{52}Cr at $10 \mu\text{g L}^{-1}$ was $3.12 \pm 0.04 \text{ V}$ (2 SD, relative standard deviation (RSD) =

0.6%) during a single measurement. The standard solutions SRM 979 and SRM 3112a with $10 \mu\text{g L}^{-1}$ of Cr were measured seven times over 8 h, with ^{52}Cr intensity only varying from 3.17 to 2.90 V with an RSD less than 4.0%, confirming excellent signal stability. In comparison with other methods to improve sensitivity and stability, such as equipping the newly developed $10^{13} \Omega$ amplifier,⁵⁴ using a high-speed mechanical booster pump,⁵⁵ and adding trifluoromethane⁵⁶ or nitrogen (N_2),⁵⁷ our method has three advantages: (1) relatively very low cost, (2) easy to operate, and (3) extendable to any other heavy metal isotopes such as Mo, Cd, etc., and elemental concentration measurement by ICP-MS. Additionally, nitrogen (N_2) introduction is also an easy way to increase sensitivity and is used in measuring some isotopes. If combining our method with introducing N_2 or trifluoromethane, as suggested by other researchers,^{56,57} it seems quite possible to obtain a high precision Cr isotope ratio at the 3 ng level or less. But this still needs further tests.

Correction for Isobaric Interferences. Since sensitivity was improved, interference was another critical factor for measuring Cr isotopes with a small amount of sample. The interferences mainly result from polyatomic ions such as $^{40}\text{Ar}^{12}\text{C}^+$, $^{40}\text{Ar}^{14}\text{N}^+$, and $^{40}\text{Ar}^{16}\text{O}^+$ on $^{52}\text{Cr}^+$, $^{54}\text{Cr}^+$, and $^{56}\text{Fe}^+$ and isobaric ions like $^{50}\text{Ti}^+$ and $^{50}\text{V}^+$ on $^{50}\text{Cr}^+$ and $^{54}\text{Fe}^+$ on $^{54}\text{Cr}^+$.⁵⁹ The former can be easily eliminated by using the medium or high resolution mode, while the latter is impossible to avoid completely via medium or high resolution. For example, a mass resolution ($m/\Delta m$, 5%, 95%) of approximately 74 000 was needed to efficiently separate the mass peaks of $^{54}\text{Fe}^+$ and $^{54}\text{Cr}^+$, yet no existing commercially available MC-ICP-MS has this ability. Previous studies have shown that the $\delta^{53}\text{Cr}$ value can shift when the $[\text{Fe} \text{ or } \text{Ti}]/[\text{Cr}]$ is high, or Fe and Ti isotopic compositions are fractionated from the standard values,^{6,9} even after the isobaric interference were subtracted based on ^{56}Fe and ^{49}Ti . In this study, Ti can be easily removed during chemical purification with a final $[\text{Ti}]/[\text{Cr}] \leq 0.04$, and thus it is negligible. However, trace Fe occasionally still remains with $[\text{Fe}]/[\text{Cr}] > 0.1$, especially for samples with low Cr content and $[\text{Fe}]/[\text{Cr}] \geq 9000$. With such high Fe, straightforward subtraction cannot bring $\delta^{53}\text{Cr}$ back to the true values, as demonstrated by doping SRM 979s with various amounts of Fe (Figure 3). The raw data were subject to interference correction before the iterative double spike data reduction algorithm, and the results are plotted in Figure 3, which shows clear errors at $[\text{Fe}]/[\text{Cr}] \geq 0.1$ due to high sensitivity in this study. The errors become significant at slightly lower ratios than those observations in previous studies ($[\text{Fe}]/[\text{Cr}] \leq 0.4$).^{6,9} Consequently, the samples have to be repurified to eliminate a tiny amount of residual Fe. However, reprocessing is not always feasible for limited samples and can introduce more blank. Alternatively, we tentatively propose a *post hoc* correction method. As shown in Figure 3a, c, and d, there is a significant linear correlation ($R^2 = 0.99$) between the $\delta^{53}\text{Cr}$ values of doped SRM 979 and $[\text{Fe}]/[\text{Cr}]$. A similar linear correlation also exists between the $\delta^{53}\text{Cr}$ of real samples and $[\text{Fe}]/[\text{Cr}]$. Thus, the empirical equation is fitted with a least-square method to be

$$\delta^{53}\text{Cr} = a \times X + b \quad (1)$$

where a is the slope, b is the intercept, representing the true Cr isotope ratio of sample. X is $[\text{Fe}]/[\text{Cr}]$, representing the variable concentration ratio of Fe to Cr; $\delta^{53}\text{Cr}$ is the measured

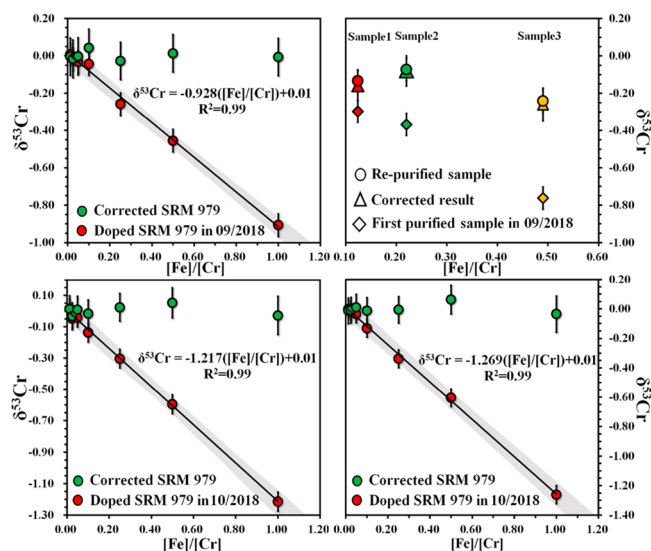


Figure 3. Assessment of the effects of Fe on Cr isotope determination. Figure 3a, c, and d show the measured and corrected results of SRM 979 doped with varying amounts of Fe. Figure 3b shows the results of geological samples. Data in Figure 3a,b were measured in the same session in September 2018, whereas data in Figure 3c and d were determined in the same session in October 2018. The gray area represents the 95% confidence interval for the fitted equation.

value after DS data reduction. Since the slope remains constant within an analytical session, the true $\delta^{53}\text{Cr}$ can be calculated:

$$\delta^{53}\text{Cr}_{i-\text{corrected}} = \delta^{53}\text{Cr} - a \times X \quad (2)$$

where $\delta^{53}\text{Cr}_{i-\text{corrected}}$ is the true $\delta^{53}\text{Cr}$. It is noted that the slope varies slightly at the different analytical sessions, but it is consistent in the same analytical session (Figure 3a–c vs Figure 3c,d).

Using this method, the corrected SRM 979 $\delta^{53}\text{Cr}$ is 0.00 ± 2 SD ($0.08\% \leq 2 \text{ SD} \leq 0.14\%$), which is within the analytical uncertainty. The uncertainties involved with this correction data are calculated to be in the range of 0.08‰ to 0.14‰ depending on the ratio variation of $[\text{Fe}]/[\text{Cr}]$ from 0.1 to 1 according to the principles of error propagation⁵⁸ (eq S1). This correction method can return the same $\delta^{53}\text{Cr}$ value in different sessions, despite different slopes. Importantly, the empirical equation can be used to correct not only for the 0‰ SRM 979 standard but also actual samples with $[\text{Fe}]/[\text{Cr}] \geq 0.1$ and $\delta^{53}\text{Cr}$ away from 0‰. For example, the $\delta^{53}\text{Cr}$ values of two shale and one plant sample (Table S4) were corrected to be $-0.16 \pm 0.08 \%$ (2 SD), $-0.06 \pm 0.08 \%$ (2 SD), and $-0.24 \pm 0.09 \%$ (2 SD), with $[\text{Fe}]/[\text{Cr}]$ at 0.12, 0.22, and 0.49, respectively. These values are in accordance with the measured results of repurified samples in the range of analytical uncertainty (Figure 3b), suggesting that the empirical equation can efficiently correct for the residual isotope drift caused by isobaric interferences that could not be completely corrected for with a standard interference subtraction procedure.

The Precision and Accuracy. SRM 979, purified BHVO-2, and SRG-1b at Cr concentrations of 3, 5, 10, 25, and $50 \mu\text{g L}^{-1}$ were repeatedly measured to evaluate precision (Figure 4). The 2 standard deviation (2 SD) precisions of SRM 979, BHVO-2 and SRG-1b were 0.07‰, 0.13‰, 0.18‰ ($n = 3$) for $3 \mu\text{g L}^{-1}$; 0.05‰, 0.06‰, and 0.08‰ ($n = 3$) for $5 \mu\text{g L}^{-1}$; and 0.03‰, 0.05‰, and 0.05‰ ($n = 3$) for $\geq 10 \mu\text{g L}^{-1}$, respectively. The precision improves with the increase of Cr

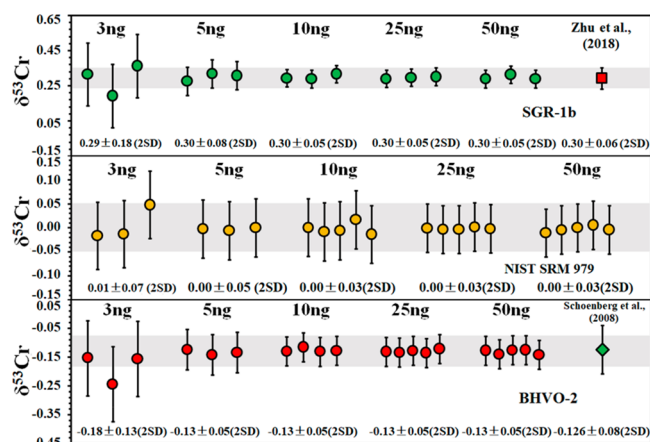


Figure 4. Comparisons of measured results for SGR-1b, SRM 979, and BHVO-2 at varying concentrations.

concentration and then levels off when Cr concentration is $\geq 10 \mu\text{g L}^{-1}$, confirming that high-precision ($2 \text{ SD} \leq 0.05\%$) Cr isotope composition can be determined at the $10 \mu\text{g L}^{-1}$ level using the improved sample introduction system. The precision obtained at $10 \mu\text{g L}^{-1}$ Cr is in excellent agreement with those reported precisions measured at $\geq 50 \mu\text{g L}^{-1}$ by MC-ICP-MS^{6,7,9} and better than 0.26% (2 SD) by MC-ICP-MS⁴³ and 0.20% (2 SD)⁴⁶ by MC-TIMS at 10 ng of Cr level.

The $\delta^{53}\text{Cr}$ values are $0.00 \pm 0.03\%$ (2 SD , $n = 15$) for SRM 979, $-0.13 \pm 0.05\%$ (2 SD , $n = 14$) for BHVO-2, $0.30 \pm 0.05\%$ (2 SD , $n = 9$) for SGR-1b, and $-0.08 \pm 0.05\%$ (2 SD , $n = 3$) for JP-1 at $[\text{Cr}] \geq 10 \mu\text{g L}^{-1}$, which agree with the corresponding values reported in the literature,^{5,8,9} confirming that high precision and accuracy can be obtained by our

method, with measuring Cr concentrations as low as $10 \mu\text{g L}^{-1}$. In addition, the $\delta^{53}\text{Cr}$ values of SRM 979, BHVO-2, and SGR-1b at $3 \mu\text{g L}^{-1}$ and $5 \mu\text{g L}^{-1}$ are $0.01 \pm 0.07\%$, $-0.18 \pm 0.13\%$, and $0.29 \pm 0.18\%$ and $0.00 \pm 0.05\%$, $-0.13 \pm 0.06\%$, and $0.30 \pm 0.08\%$ (Figure 4), respectively, which are the same as previously reported values within the uncertainty range. These results indicate that accurate $\delta^{53}\text{Cr}$ values can still be obtained using Cr concentration as low as $3 \mu\text{g L}^{-1}$.

The $\delta^{53}\text{Cr}$ Values of Geological Reference Materials (GRMs). The $\delta^{53}\text{Cr}$ values for 19 GRMs are reported for the first time, and their $\delta^{53}\text{Cr}$ values range from -0.44% to 0.49% (Table 2). After excluding three isotopically fractionated samples, GSS-7 ($-0.44 \pm 0.02\%$; 2 SD , $n = 4$), GSS-4 ($0.48 \pm 0.02\%$; 2 SD , $n = 4$), and GSD-10 ($0.49 \pm 0.05\%$; 2 SD , $n = 8$), that were taken from the weathered basalt and carbonate units, the average $\delta^{53}\text{Cr}$ value of the GRMs set is $-0.11 \pm 0.16\%$ (2 SD , $n = 11$) for soils and stream sediment samples and $-0.15 \pm 0.05\%$ (2 SD , $n = 5$) for igneous and sedimentary rocks, which are within uncertainty, the same as for the upper continental crust ($-0.10 \pm 0.10\%$)⁹ and the bulk silicate earth ($-0.124 \pm 0.101\%$).⁵ Given that previously used siliciclastic reference materials (e.g., SDO-1, which has been discontinued) have $\delta^{53}\text{Cr}$ values similar to the bulk silicate earth, we therefore suggest that GSS-7, GSS-4, and GSD-10 could serve as the potential reference materials with fractionated $\delta^{53}\text{Cr}$ for interlaboratory comparisons.

As shown in Table 2, the $\delta^{53}\text{Cr}$ of GRMs determined at different Cr concentrations are compared. The $\delta^{53}\text{Cr}$ obtained at $10 \mu\text{g L}^{-1}$ is identical to that at $25 \mu\text{g L}^{-1}$ and $50 \mu\text{g L}^{-1}$, and the 2 SDs are lower than 0.06% ($n = 4$ or 5). The results further demonstrate that a highly precise and accurate Cr isotope ratio can be easily determined at the 10 ng level by MC-ICP-MS.

Table 2. Results of Environmental and Geological Reference Materials at Varied Concentrations

sample name	sample type	$\delta^{53}\text{Cr}$ (‰)					mean $\pm 2 \text{ SD}$ (‰) ^a
		10 ng	25 ng	50 ng	50 ng	50 ng	
GSR-1	granite	-0.17	-0.14	-0.13	-0.13		-0.14 ± 0.03
GSR-2	andesite	-0.11	-0.15	-0.14	-0.12	-0.15	-0.13 ± 0.03
BHVO-2	basalt	-0.13	-0.13	-0.14	-0.13	-0.13	-0.13 ± 0.05
JP-1	peridotite	-0.08	-0.09	-0.10	-0.09		-0.09 ± 0.02
GSR-4	quartz sandstone	-0.15	-0.17	-0.12	-0.15	-0.16	-0.15 ± 0.03
GSR-5	shale	-0.14	-0.17	-0.17	-0.16	-0.17	-0.16 ± 0.02
SGR-1b	shale	0.30	0.30	0.29	0.32	0.29	0.30 ± 0.02
GSR-6	limestone	-0.14	-0.11	-0.12	-0.13		-0.13 ± 0.03
GSS-1	soil	-0.16	-0.17	-0.14	-0.15	-0.16	-0.16 ± 0.02
GSS-2	soil	-0.13	-0.12	-0.13	-0.10	-0.12	-0.12 ± 0.02
GSS-3	soil	-0.19	-0.19	-0.14	-0.16	-0.14	-0.16 ± 0.05
GSS-4	soil	0.46	0.49	0.48	0.48	0.50	0.48 ± 0.02
GSS-5	soil	-0.04	0.01	-0.01	-0.01	0.00	-0.01 ± 0.03
GSS-6	soil	-0.13	-0.14	-0.17	-0.18	-0.14	-0.16 ± 0.04
GSS-7	soil	-0.45	-0.44	-0.43	-0.45	-0.42	-0.44 ± 0.02
ESS-1	soil	-0.13	-0.12	-0.14	-0.13		-0.13 ± 0.01
GSD-1	stream sediment	-0.15	-0.14	-0.17	-0.15	-0.16	-0.15 ± 0.02
GSD-3	stream sediment	-0.23	-0.18	-0.19	-0.19	-0.19	-0.20 ± 0.03
GSD-9	stream sediment	-0.04	-0.13	-0.08	-0.07	-0.10	-0.08 ± 0.06
GSD-10	stream sediment	0.50	0.50	0.49	0.51	0.44	0.49 ± 0.05
repeat		0.52	0.48	0.47	0.49	0.47	0.49 ± 0.03
GSD-11	stream sediment	-0.14	-0.13	-0.12	-0.11	-0.15	-0.13 ± 0.02
GSD-12	stream sediment	0.12	0.09	0.11	0.12	0.08	0.10 ± 0.03

^aThe average and 2 SD are calculated using all data measured at various Cr masses.

As instrument sensitivity and stability can be significantly improved, as demonstrated in this paper, the procedural Cr blank becomes the next limiting factor for obtaining high-precision Cr isotope composition in extremely low-Cr samples. Because of the wide range of sample types investigated in this paper, we adopted a universal purification method developed in Zhu et al.,⁹ which has a relatively high Cr blank (~0.8 ng). Therefore, we processed sample amounts equivalent to 200–300 ng of Cr so that blank Cr is <0.4% of the sample Cr. However, if the blank can be reduced to be <0.2 ng for most geological and environmental samples, as described in Bonnand et al.⁶ and Li et al.⁴⁵ for carbonate samples, the Cr isotope system can be applied to a significantly wider range of samples. Therefore, further work should be conducted to develop a better purification protocol that can cover a wide range of sample types with low Cr blank.

CONCLUSION

Using an improved Aridus II with a cooled (5 °C) waste gas condensation chamber as the sample introduction system, $\delta^{53}\text{Cr}$ can be determined at a 10 ng level with high accuracy and precision (better than 0.06‰, 2 SD) by double spike MC-ICP-MS. Shifts of measured $\delta^{53}\text{Cr}$ due to isobaric Fe interference greater than the range where the normal interference correction is accurate can be corrected for with a secondary correction—a linear equation calibrated for each analytical session. The $\delta^{53}\text{Cr}$ values for previously used GRMs measured at various concentrations (3, 5, 10, 25, 50 $\mu\text{g L}^{-1}$) are consistent with previous measurements within analytical uncertainty. Using our method, we also reported the $\delta^{53}\text{Cr}$ of 19 new GRMs, among which GSS-4, GSS-7, and GSD-10 have fractionated Cr isotope compositions compared to previously used unfractionated reference materials, and thus are good candidates for interlaboratory comparisons. If a suitable method with a lower total blank can be developed to cover a wide range of sample types, highly precise and accurate Cr isotope data for very low-Cr samples can be determined readily, significantly expanding the application of the Cr isotope proxy.

ASSOCIATED CONTENT

Supporting Information

The Supporting Information is available free of charge at <https://pubs.acs.org/doi/10.1021/acs.analchem.9b04704>.

Tables S1, S2, S3, and S4 and detailed uncertainty calculation (eq S1) (PDF)

AUTHOR INFORMATION

Corresponding Author

*E-mail: jmzhu@cugb.edu.cn.

ORCID

Jian-Ming Zhu: 0000-0003-4977-6072

Notes

The authors declare no competing financial interest.

ACKNOWLEDGMENTS

This work was funded by the National Natural Science Foundation of China (Nos. U1612441 and 41673017), the National Key Basic Research Program of China (2014CB238903) and MOST Special Fund from the State Key Laboratory of Geological Processes and Mineral

Resources, China University of Geosciences (MSFGPMR201812 and 201814). The authors thank two anonymous reviewers for their insightful suggestions.

REFERENCES

- (1) de Laeter, J. R.; Bohlke, J. K.; De Bièvre, P.; Hidaka, H.; Peiser, H. S.; Rosman, K. J. R.; Taylor, P. D. P. *Pure Appl. Chem.* **2003**, *75*, 683–800.
- (2) Shields, W. R.; Murphy, T. J.; Catanzaro, E. J.; Garner, E. L. *J. Res. Natl. Bur. Stand., Sect. A* **1966**, *70A*, 193–197.
- (3) Ball, J. W.; Bassett, R. L. *Chem. Geol.* **2000**, *168*, 123–134.
- (4) Ellis, A. S.; Johnson, T. M.; Bullen, T. D. *Science* **2002**, *295*, 2060–2062.
- (5) Schoenberg, R.; Zink, S.; Staubwasser, M.; von Blanckenburg, F. *Chem. Geol.* **2008**, *249*, 294–306.
- (6) Bonnand, P.; Parkinson, I. J.; James, R. H.; Karjalainen, A.-M.; Fehr, M. A. *J. Anal. At. Spectrom.* **2011**, *26*, 528–535.
- (7) Shen, J.; Liu, J.; Qin, L.; Wang, S.-J.; Li, S.; Xia, J.; Ke, S.; Yang, J. *Geochem., Geophys., Geosyst.* **2015**, *16*, 3840–3854.
- (8) Wang, X.; Planavsky, N. J.; Reinhard, C. T.; Zou, H.; Ague, J. J.; Wu, Y.; Gill, B. C.; Schwarzenbach, E. M.; Peucker-Ehrenbrink, B. *Chem. Geol.* **2016**, *423*, 19–33.
- (9) Zhu, J.-M.; Wu, G.; Wang, X.; Han, G.; Zhang, L. *J. Anal. At. Spectrom.* **2018**, *33*, 809–821.
- (10) Schiller, M.; Van Kooten, E.; Holst, J. C.; Olsen, M. B.; Bizzarro, M. *J. Anal. At. Spectrom.* **2014**, *29*, 1406–1416.
- (11) Frei, R.; Gaucher, C.; Poulton, S. W.; Canfield, D. E. *Nature* **2009**, *461*, 250–253.
- (12) Reinhard, C. T.; Planavsky, N. J.; Wang, X.; Fischer, W. W.; Johnson, T. M.; Lyons, T. W. *Earth Planet. Sci. Lett.* **2014**, *407*, 9–18.
- (13) Cole, D. B.; Reinhard, C. T.; Wang, X.; Gueguen, B.; Halverson, G. P.; Gibson, T.; Hodgskiss, M. S. W.; McKenzie, N. R.; Lyons, T. W.; Planavsky, N. J. *Geology* **2016**, *44*, 555–558.
- (14) D'Arcy, J.; Gilleaudeau, G. J.; Peralta, S.; Gaucher, C.; Frei, R. *Chem. Geol.* **2017**, *448*, 1–12.
- (15) Izbicki, J. A.; Ball, J. W.; Bullen, T. D.; Sutley, S. J. *Appl. Geochem.* **2008**, *23*, 1325–1352.
- (16) Izbicki, J. A.; Bullen, T. D.; Martin, P.; Schroth, B. *Appl. Geochem.* **2012**, *27*, 841–853.
- (17) Basu, A.; Johnson, T. M.; Sanford, R. A. *Geochim. Cosmochim. Acta* **2014**, *142*, 349–361.
- (18) Kazakis, N.; Kantiranis, N.; Kalaitzidou, K.; Kaprara, E.; Mitrakas, M.; Frei, R.; Vargemezis, G.; Tsourlos, P.; Zouboulis, A.; Filippidis, A. *Sci. Total Environ.* **2017**, *593–594*, 552–566.
- (19) Kanagaraj, G.; Elango, L. *Chemosphere* **2019**, *220*, 943–953.
- (20) Farkaš, J.; Frýda, J.; Paulukat, C.; Hathorne, E. C.; Matoušková, Š.; Rohovec, J.; Frýdová, B.; Francová, M.; Frei, R. *Earth Planet. Sci. Lett.* **2018**, *498*, 140–151.
- (21) Pereira, N. S.; Voegelin, A. R.; Paulukat, C.; Sial, A. N.; Ferreira, V. P.; Frei, R. *Geobiology* **2016**, *14*, 54–67.
- (22) Bonnand, P.; James, R. H.; Parkinson, I. J.; Connelly, D. P.; Fairchild, I. J. *Earth Planet. Sci. Lett.* **2013**, *382*, 10–20.
- (23) Frei, R.; Gaucher, C.; Døssing, L. N.; Sial, A. N. *Earth Planet. Sci. Lett.* **2011**, *312*, 114–125.
- (24) Ludwig, K. A.; Kelley, D. S.; Butterfield, D. A.; Nelson, B. K.; Früh-Green, G. *Geochim. Cosmochim. Acta* **2006**, *70*, 3625–3645.
- (25) Holmden, C.; Jacobson, A. D.; Sageman, B. B.; Hurtgen, M. T. *Geochim. Cosmochim. Acta* **2016**, *186*, 277–295.
- (26) Scheiderich, K.; Amini, M.; Holmden, C.; Francois, R. *Earth Planet. Sci. Lett.* **2015**, *423*, 87–97.
- (27) Nakayama, E.; Tokoro, H.; Kuwamoto, T.; Fujinaga, T. *Nature* **1981**, *290*, 768–770.
- (28) Murray, J. W.; Spell, B.; Paul, B. *Springer US* **1983**, 643–669.
- (29) Bruggmann, S.; Scholz, F.; Kläbe, R. M.; Canfield, D. E.; Frei, R. *Geochim. Cosmochim. Acta* **2019**, *257*, 224–242.
- (30) Goring-Harford, H. J.; Klar, J. K.; Pearce, C. R.; Connelly, D. P.; Achterberg, E. P.; James, R. H. *Geochim. Cosmochim. Acta* **2018**, *236*, 41–59.

- (31) Paulukat, C.; Gilleaudeau, G. J.; Chernyavskiy, P.; Frei, R. *Chem. Geol.* **2016**, *444*, 101–109.
- (32) Rimmelzwaal, S. R. C.; Sadekov, A. Y.; Parkinson, I. J.; Schmidt, D. N.; Titelboim, D.; Abramovich, S.; Roepert, A.; Kienhuis, M.; Polerecky, L.; Goring-Harford, H.; Kimoto, K.; Allen, K. A.; Holland, K.; Stewart, J. A.; Middelburg, J. J. *Earth Planet. Sci. Lett.* **2019**, *515*, 100–111.
- (33) Wang, X.; Glass, J. B.; Reinhard, C. T.; Planavsky, N. J. *Geochem., Geophys., Geosyst.* **2019**, *20*, 2499–2514.
- (34) Wu, W.; Wang, X.; Reinhard, C. T.; Planavsky, N. J. *Chem. Geol.* **2017**, *456*, 98–111.
- (35) Li, H.; Ling, M.-x.; Li, C.-y.; Zhang, H.; Ding, X.; Yang, X.-y.; Fan, W.-m.; Li, Y.-l.; Sun, W.-d. *Lithos* **2012**, *150*, 26–36.
- (36) Foden, J.; Sossi, P. A.; Wawryk, C. M. *Lithos* **2015**, *212–215*, 32–44.
- (37) Wu, H.; He, Y.; Teng, F.-Z.; Ke, S.; Hou, Z.; Li, S. *Geochim. Cosmochim. Acta* **2018**, *222*, 671–684.
- (38) Staudigel, H.; Albarède, F.; Blichert-Toft, J.; Edmond, J.; McDonough, B.; Jacobsen, S. B.; Keeling, R.; Langmuir, C. H.; Nielsen, R. L.; Plank, T.; Rudnick, R.; Shaw, H. F.; Shirey, S.; Veizer, S.; White, W. *Chem. Geol.* **1998**, *145*, 153–159.
- (39) Moos, S. B.; Boyle, E. A. *Chem. Geol.* **2019**, *511*, 481–493.
- (40) Nutman, A. P.; Bennett, V. C.; Friend, C. R. L.; Van Kranendonk, M. J.; Chivas, A. R. *Nature* **2016**, *537*, 535–538.
- (41) Hoffman, P. F.; Kaufman, A. J.; Halverson, G. P.; Schrag, D. P. *Science* **1998**, *281*, 1342–1346.
- (42) Shen, B.; Jacobsen, B.; Lee, C. T. A.; Yin, Q.-Z.; Morton, D. M. *Proc. Natl. Acad. Sci. U. S. A.* **2009**, *106*, 20652–20657.
- (43) Wang, X. L.; Planavsky, N. J.; Hull, P. M.; Tripathi, A. E.; Zou, H. J.; Elder, L.; Henahan, M. *Geobiology* **2017**, *15*, 51–64.
- (44) Foster, G. L.; Ni, Y.; Haley, B.; Elliott, T. *Chem. Geol.* **2006**, *230*, 161–174.
- (45) Li, C.-F.; Feng, L.-J.; Wang, X.-C.; Wilde, S. A.; Chu, Z.-Y.; Guo, J.-H. *J. Anal. At. Spectrom.* **2017**, *32*, 1938–1945.
- (46) Li, C.-F.; Feng, L.-J.; Wang, X.-C.; Chu, Z.-Y.; Guo, J.-H.; Wilde, S. A. *J. Anal. At. Spectrom.* **2016**, *31*, 2375–2383.
- (47) Xiao, G.; Jones, R. L.; Saunders, D.; Caldwell, K. L. *Radiat. Prot. Dosim.* **2014**, *162*, 618–24.
- (48) CETAC Aridus II Desolvating Nebulizer System Operator's Manual, Manual Part Number 480144 Rev 3; CETAC Technologies: Omaha, NE, 2013.
- (49) Lesniewski, J. E.; Zheng, K.; Lecchi, P.; Dain, D.; Jorabchi, K. *Anal. Chem.* **2019**, *91*, 3773–3777.
- (50) Pontér, S.; Pallavicini, N.; Engström, E.; Baxter, D. C.; Rodushkin, I. J. *Anal. At. Spectrom.* **2016**, *31*, 1464–1471.
- (51) Halicz, L.; Yang, L.; Teplyakov, N.; Burg, A.; Sturgeon, R.; Kolodny, Y. *J. Anal. At. Spectrom.* **2008**, *23*, 1622–1627.
- (52) Walder, A. J.; Koller, D.; Reed, N. M.; Hutton, R. C.; Freedman, P. A. *J. Anal. At. Spectrom.* **1993**, *8*, 1037–1041.
- (53) Hu, Z.; Liu, Y.; Gao, S.; Xiao, S.; Zhao, L.; Günther, D.; Li, M.; Zhang, W.; Zong, K. *Spectrochim. Acta, Part B* **2012**, *78*, 50–57.
- (54) Koornneef, J. M.; Bouman, C.; Schwieters, J. B.; Davies, G. R. *Anal. Chim. Acta* **2014**, *819*, 49–55.
- (55) Yuan, H.; Bao, Z.; Chen, K.; Zong, C.; Chen, L.; Zhang, T. *J. Anal. At. Spectrom.* **2019**, *34*, 1011–1017.
- (56) Larsen, K. K.; Wielandt, D.; Schiller, M.; Bizzarro, M. *J. Chromatogr. A* **2016**, *1443*, 162–74.
- (57) Craig, J. M.; Beauchemin, D. *J. Anal. At. Spectrom.* **1992**, *7*, 937–942.
- (58) Phillips, D. L.; Gregg, J. W. *Oecologia* **2001**, *127*, 171–179.